Electronic Supplementary Information

A novel split mode TFBAR devices for quantitative measurements of prostate specific antigen in a small sample of whole blood.

Ewelina Wajs,[*a†] Girish Rughoobur,[b] Keith Burling,[c] Anne George,[d] Andrew J. Flewitt[#a] and VJ. Gnanapragasam[d,e,f#]

[a] *Electrical Engineering, University of Cambridge, 9 JJ Thomson Avenue, Cambridge, CB3 0FA, UK.*

[b] *Microsystems Technology Laboratories, Massachusetts Institute of Technology, 60 Vassar Street, Cambridge, MA 02139, USA.*

[c] *NIHR Core Biochemical Assay Laboratory (CBAL), Cambridge University Hospitals NHS Foundation Trust*

[d] *Cambridge Urology Translational Research and Clinical Trials, Addenbrookes Hospital*

[e] *Academic Urology Group, Department of Surgery, Cambridge University Hospitals NHS Foundation Trust and University of Cambridge*

[f] *CRUK Cambridge Cancer Centre, Cambridge Biomedical Campus, University of Cambridge*

[†] *Present address: ICFO, Mediterranean Technology Park, Av. Carl Friedrich Gauss 3, 08860 Castelldefels (Barcelona), Spain.*

* Corresponding Author: ewelina.wajs@icfo.eu

[#] Joint Senior Authors

1. Photographs of the TFBAR biosensor measurement setup.

The Figure S1 A shows an optical image of the fabricated TFBAR devices in a 5 × 5 array layout with enlarged view of 4 devices. Each of the TBFAR was measured separately using 150 µm pitch ground-signal-ground (GSG) probes with a customised holder for the probe and the device (Figure S1 B). The biofunctionalisation steps of the TFBAR devices and PSA measurements are explained in the main manuscript in the experimental section.

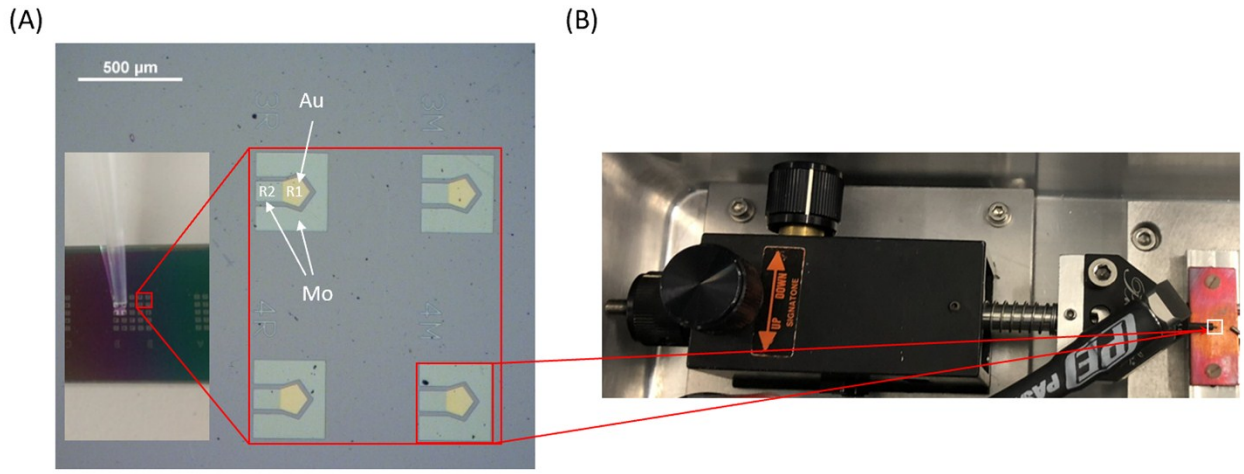

Figure S1. (A) *A photograph of the split-mode TFBAR devices with the functional gold layer only on a pentagonal section of the molybdenum top electrode, illustrating the regions corresponding to the first (R1) and second (R2) resonances; enlarged is a view of the 4 TFBAR devices;* ***(B)*** *A measurement setup with a 150 µm pitch ground-signal-ground (GSG) probe and customised holder for the probe and the device.*

2. Experimental Section

2.1 Materials

Thiol molecule, 11-mercaptoundecanoic acid 98% (11-MUA) was purchased from ChemCruz; 6-mercapto-1-hexanol, ethanolamine, 1-ethyl-3-(3-dimethylaminopropyl) carbodiimide hydrochloride (EDC), N-hydroxysuccinimide (NHS), human serum albumin and prostate specific antigen from human semen were purchased from Sigma-Aldrich (Merck); Anti-PSA polyclonal capture antibody was purchased from GeneTech; monoclonal anti-PSA antibody was purchased from HyTest; K2EDTA samples were taken from suitable subjects following consent under the DIAMOND study (IRAS ID-158493). For buffered measurements, PSA antigen was diluted in phosphate buffer (pH 7.2) to the desired concentrations, whilst EDTA whole blood samples containing various concentrations of PSA antigen were used as received.

Devices were pre-equilibrated with using clean PBS buffer solutions. Thus, prior to each experiment a reference was measured with clean PBS buffer solution, what served as a baseline for next biomolecules attachment.

2.2 Preparation of the humidity chamber.

To avoid drying of the spotted slides we prepared a special humidity chamber. For this we prepared a suitable sealable container (a plastic food container) by adding a tray to hold the slides and underneath this, a large Petri dish. We filled the Petri dish with steaming hot water 30 min prior to use. After 30 min

the air was saturated with water and have cooled to room temperature. The humid chamber was then ready for use. A new chamber was prepared for each batch of slides and in advance. Slides could be incubated for the required amount of time without drying and with the relative humidity between 65% - 75% at 20°C, which was checked with a small humidity meter.

2.3 TFBAR measurements.

After each functionalisation step, the change in the frequency was monitored by measuring the real part of the electrical admittance (*Y*) in the frequency range from 0.5 GHz to 3.0 GHz and by calculating the increase in the distance of the two resonant frequencies $\Delta(f_2 - f_1)$. This allowed to ensure effectiveness of surface modifications. Finally, samples of PSA in PBS buffer were measured and resulted in a calibration plot (Figure 2B in the main manuscript), which was then used for PSA antigen concentrations determination in a real blood samples from patients (Table 1 in the main manuscript).

2.4 Optimised Immunoassay Parameters

Prior to the development of a calibration plot for PSA, an optimal concentration of thiol molecules (11-MUA) was determined by using consistent concentration of a polyclonal anti-PSA capture antibody at 0.5 mg mL^{-1} (Figure S2). First, the formation of SAMs on the TFBAR devices was done by immersing them in ethanolic solution of 11-MUA at different concentrations (0.5 mM, 5 mM, 50 mM and 100 mM), overnight at 4 °C. At the end of the incubation time each device was thoroughly rinsed with ethanol to remove excess of the unattached thiol molecules and dried with N_2. The sensor response to the attachment of the thiol molecules (11-MUA) to the gold surface was monitored again by measuring the real part *Y* in the spectral range from 0.5 GHz to 3.0 GHz and calculating $\Delta(f_2 - f_1)$; this increase is observed as the mass sensitive frequency (f_1) shifts towards lower frequencies because of more molecules being attached to the gold surface of the TFBAR device. Next, 0.1 M solution of blocking molecule (6-mercapto-1-hexanol) was used to ensure a full surface coverage and minimise non-specific interactions. Anti-PSA antibody was used in excess to ensure the maximum attachment to the activated thiol molecules – SAM. As can be seen on the Figure S2 the maximum signal with both layers (thiols + anti-PSA antibody) was observed at 5 mM thiol concentration and therefore this was used for our experiments. The sample volume was at 10 μL per spot, which was enough to fully cover all the active area on the chip.

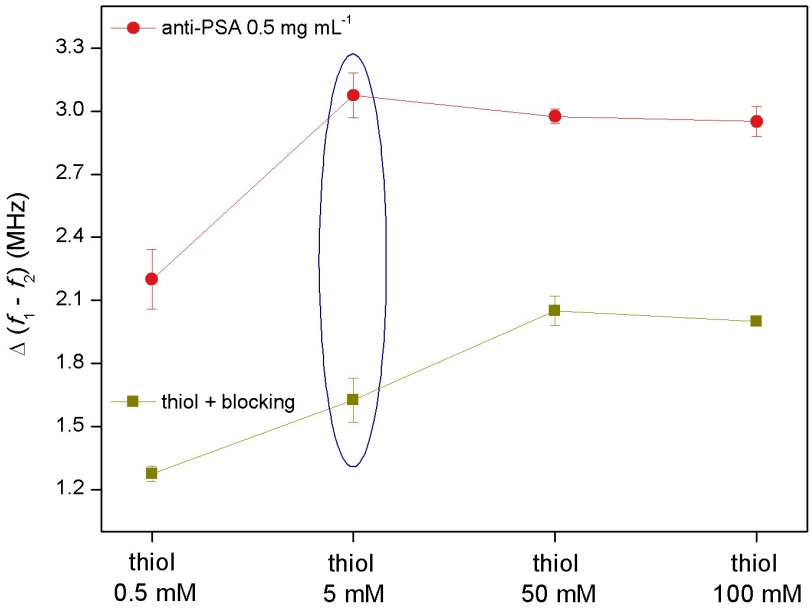

Figure S2. *Optimisation of the thiol concentration on the gold surface for the maximum attachment of the polyclonal capture antibody. An optimal concentration is circled.*

3. Testing reusability of the TFBAR modified devices

The reusability of these devices was established by treatment (cleaning) with argon plasma for 5 minutes using reactive ion etching (RIE). The modified gold surface of the TFBAR was treated with argon plasma at 50 W power and 50 sccm of argon and 150 mTorr pressure to remove all the organic material from its surface. The devices were checked by measuring the real part of the *Y* (Figure S3) to ascertain performance recovery. As can be seen with SAM deposition on the gold surface, the distance between $\Delta(f_2 - f_1)$ increased but after argon plasma treatment, it returned to the initial position (2). However, it is noticeable that the shift was slightly larger, and it can be attributed to etching some of the gold due to ion bombardment from the TFBAR surface during cleaning. Nonetheless, this experiment shows the possibility for re-using these devices, therefore significantly reducing cost of such biosensor. In fact, cleaned devices were subsequently re-used in our work.

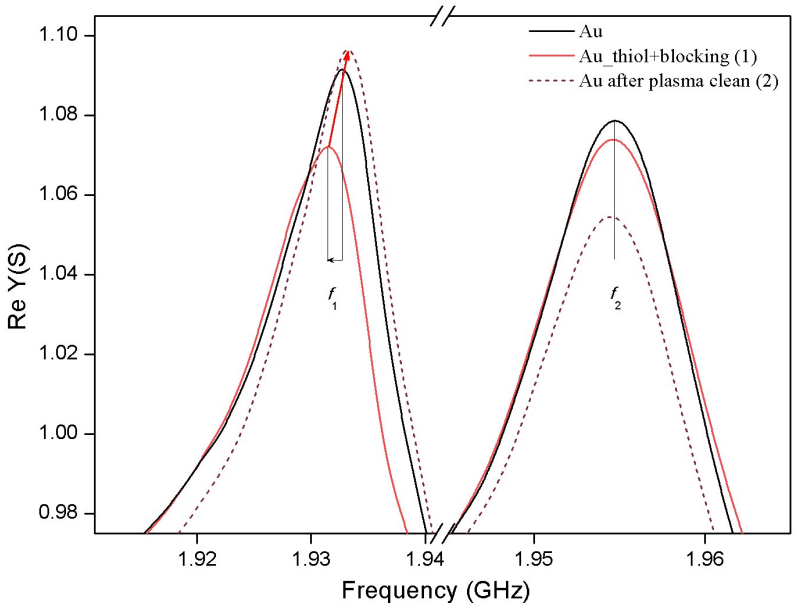

Figure S3. *The increase in the difference between the two resonances* $\Delta(f_2 - f_1)$ *observed in TFBAR device due to attachment of thiol molecules onto gold surface; Au_thiol+blocking (1); after treatment with argon plasma, the mass sensitive mode* (f_1) *showing shift towards higher frequencies due to detachment of thiol molecules from the gold surface (2).*

4. Specificity and selectivity of the fabricated TFBAR biosensor

Specificity of the surface of TFBAR biosensor was evaluated in the absence of anti-PSA antibody on SAM modified electrode arrays. Tracking of the attachment of thiol molecules to the gold surface on the TFBAR device was done by simply calculating the increase in the distance of the two resonant frequencies $\Delta(f_2 - f_1)$. This increase was observed as the mass sensitive frequency (f_1) shifted towards lower frequencies because of molecules being attached to the gold surface of the TFBAR device (as shown in Figure S4, Au_thiol + blocking (1)). The concentration of thiols: 11-MUA and blocking was at 5 mM and 0.1 M, respectively. However, in this experiment no anti-PSA antibody was attached to the SAM layer on TFBAR surface and therefore no further shift towards lower frequencies was observed (Figure S4, Au_ thiol + blocking_NO anti-PSA (2)). In this step the devices were incubated only with the clean PBS buffer solution. Thus, no antigen detection was possible and similarly no shift was observed after the incubation with PSA solution at high concentrations (10 ng mL^{-1}) (Figure S4, Au_ thiol + blocking_NO anti-PSA_PSA antigen (3)). This demonstrates a very high specific binding of the PSA antigen to anti-PSA antibody only and not to the surface of the sensor.

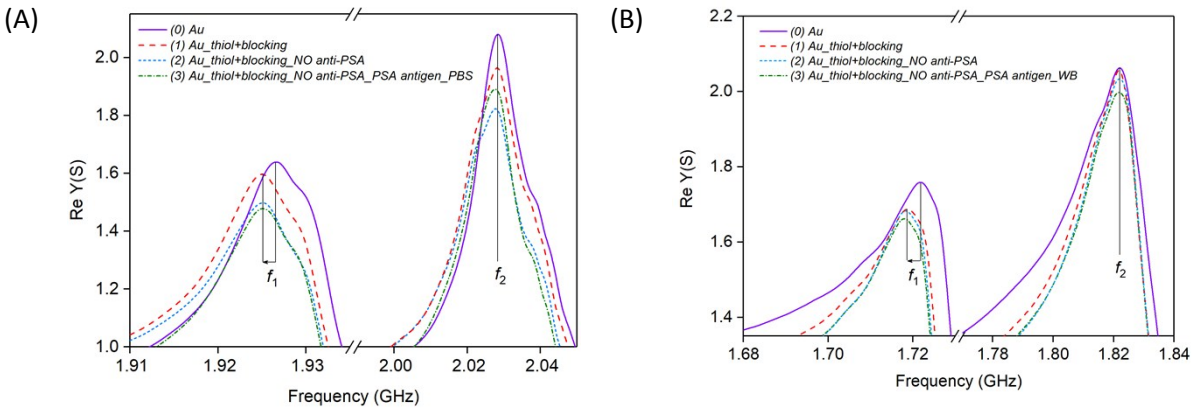

Figure S4. *Specificity of the modified surface of TFBAR biosensor for PSA, evaluated in the absence of anti-PSA capture antibody in PBS (A) and in the whole blood sample (B). The increase in the difference between the two resonant frequencies* $\Delta(f_2 - f_1)$ *observed in TFBAR device due to attachment of thiol molecules onto gold surface (0), Au_thiol+blocking (1); no shift observed without anti-PSA antibody attachment, Au_thiol+blocking_NO anti-PSA (2) and no shift observed for the PSA antigen detection, Au_thiol+blocking_NO anti-PSA_PSA antigen (3).*

To further test selectivity of the TFBAR biosensor the effect of a potentially interfering entities present in the blood samples was investigated in the presence of a human serum albumin at a concentration of 50 mg mL^{-1}. Buffered and the whole blood samples were spiked with 9 ng mL^{-1} of PSA antigen and it was found to be 9.35 ng mL^{-1} and 9.53 ng mL^{-1}, respectively. The signal recovery of PSA was calculated to be 104% in buffered and 106% in the whole blood samples, according to the equation:

$$\%\, recovery = \frac{C\ spiked\ sample - C\ unspiked\ sample}{C\ added} \times 100$$

In both cases the signal recovery was very close to 100%, further confirming that the TFBAR biosensors are selective and specific for the detection of PSA antigen.

The possible effect of the serum matrix on target detection using the TFBAR biosensor was also studied by spiking blood samples with different amounts of PSA antigen (Table S1).

Table S1. TFBAR biosensor signal recovery (%) for added amounts of PSA antigen to the whole blood samples.

Added PSA (ng mL^{-1})	Found PSA (ng mL^{-1})	Recovery of PSA (%)
3.0	3.32	110
5.0	5.35	106
7.0	7.35	105

As can be seen, the TFBAR biosensor was able to detect the target analyte (PSA antigen) in a complex matrix like blood with signal recovery near 100%, showing the applicability of the system to the analysis of a real clinical samples.

5. The TFBAR spectra changes with increasing target (PSA antigen) concentration.

The Figure S5 (A-J) demonstrates an example of the changes in the resonant frequency with increasing target concentrations. There is a visible shift of the first resonant frequency (f_1) with increasing PSA antigen concentration due to more molecules being attached to the active Au surface area of the TFBAR device. For each measurement the difference $\Delta(f_2 - f_1)$ was calculated and results plotted to obtain a calibration curve (see Figure S6 in SI and Figure 2B in the main manuscript).

A)

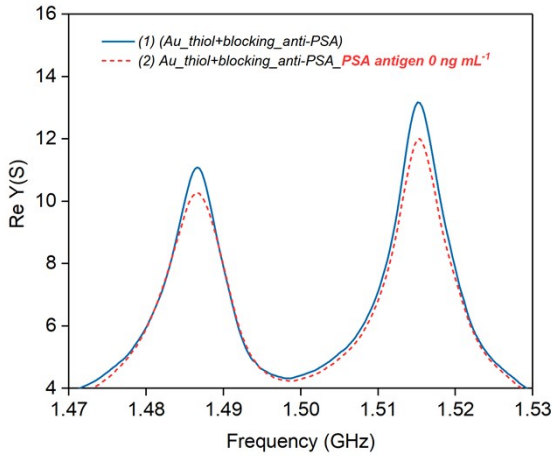
(1) (Au_thiol+blocking_anti-PSA)
(2) Au_thiol+blocking_anti-PSA_PSA antigen 0 ng mL-1
Re Y(S)
Frequency (GHz)

B)

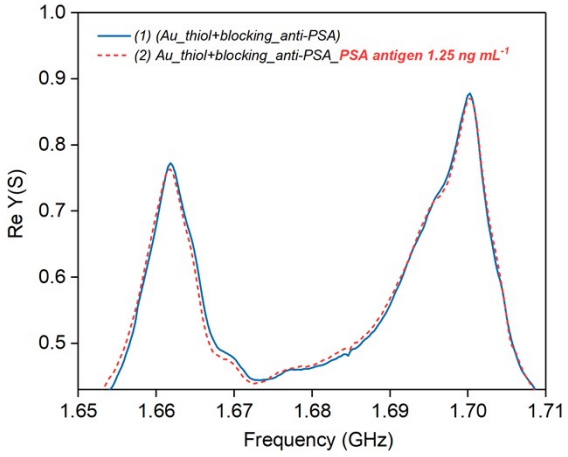
(1) (Au_thiol+blocking_anti-PSA)
(2) Au_thiol+blocking_anti-PSA_PSA antigen 1.25 ng mL-1
Re Y(S)
Frequency (GHz)

C)

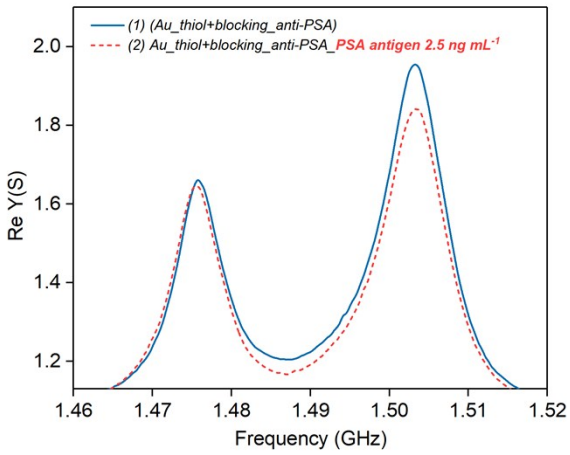
(1) (Au_thiol+blocking_anti-PSA)
(2) Au_thiol+blocking_anti-PSA_PSA antigen 2.5 ng mL-1
Re Y(S)
Frequency (GHz)

D)

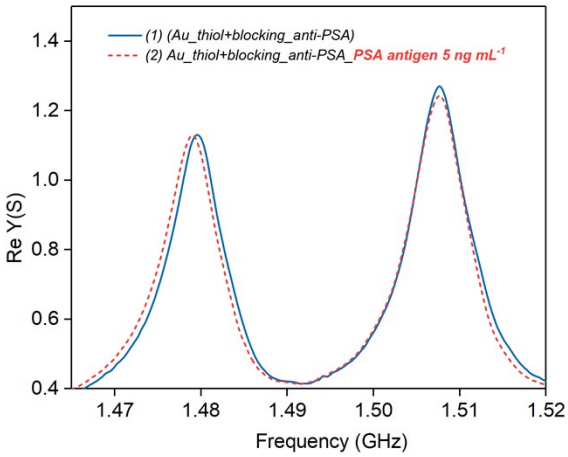
(1) (Au_thiol+blocking_anti-PSA)
(2) Au_thiol+blocking_anti-PSA_PSA antigen 5 ng mL-1
Re Y(S)
Frequency (GHz)

E)

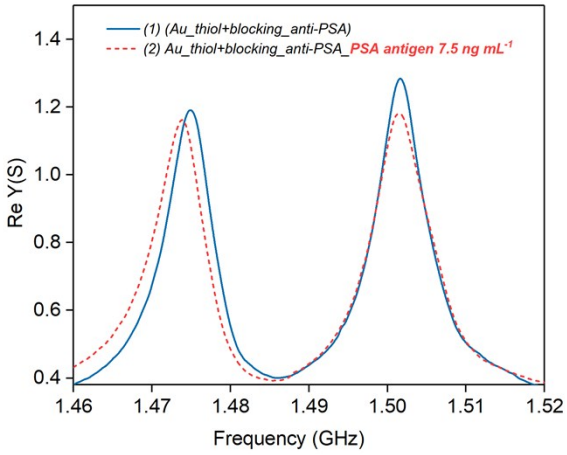
(1) (Au_thiol+blocking_anti-PSA)
(2) Au_thiol+blocking_anti-PSA_PSA antigen 7.5 ng mL-1
Re Y(S)
Frequency (GHz)

F)

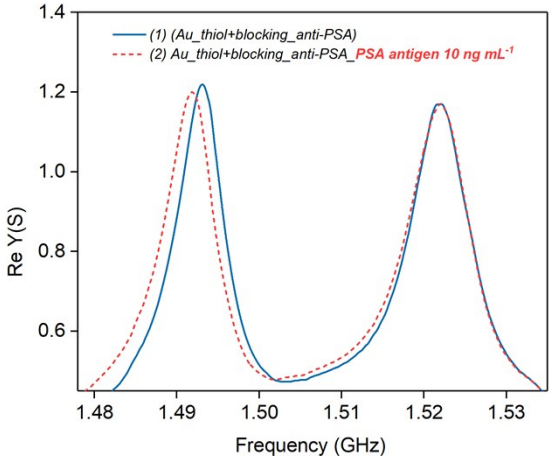
(1) (Au_thiol+blocking_anti-PSA)
(2) Au_thiol+blocking_anti-PSA_PSA antigen 10 ng mL-1
Re Y(S)
Frequency (GHz)

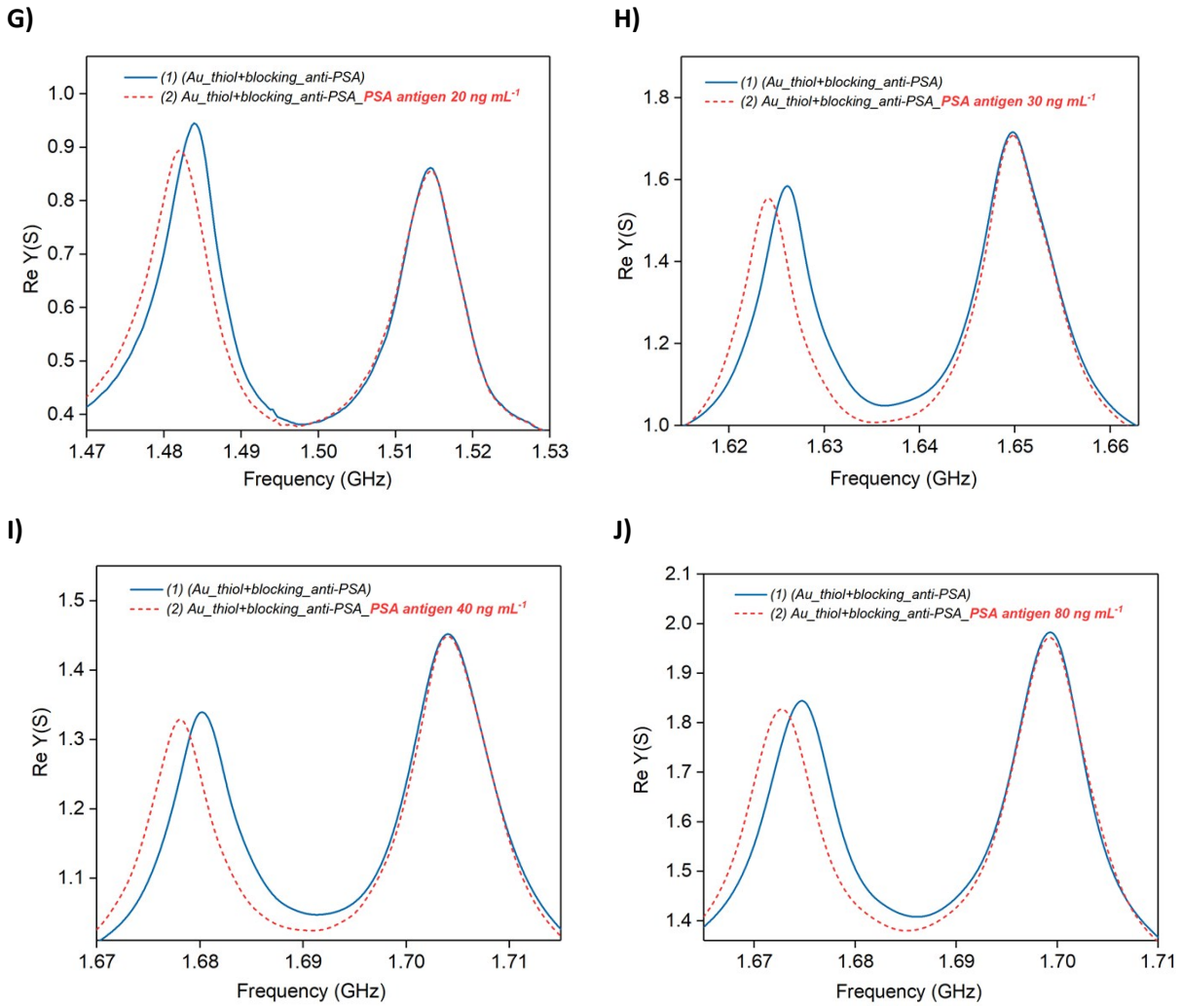

Figure S5. *The TFBAR spectra changes with increasing target (PSA antigen) concentration from 0 to 80 ng mL^{-1}.*

6. A plot demonstrating a wide concentration range of PSA antigen detection obtained with TFBAR measurements.

In this experiment we present a detection of a wide concentration range of PSA antigen (0 – 80 ng mL^{-1}) with the TFBAR devices. As it can be seen the saturation of TFBAR devices is already visible with the concentrations above 20 ng mL^{-1} of total PSA antigen. However, as it is explained in the main manuscript in the Results and discussion section, the detection of lower ranges of the total PSA (0 to 10 ng mL^{-1}) are clinically relevant and they are of a high importance for medical diagnostics. Therefore, this range was used for the subsequent calibration plot (Figure 2B in the main manuscript) and for later identification of the unknown whole blood samples.

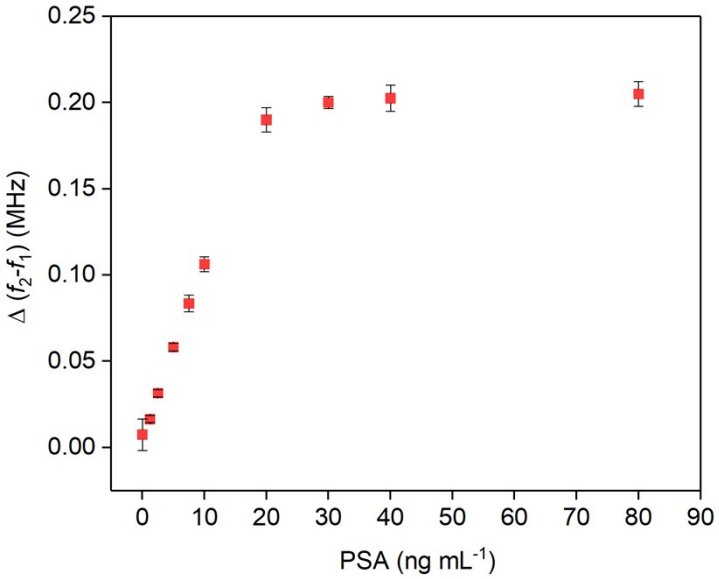

Figure S6. *A plot demonstrating the changes in $\Delta(f_2 - f_1)$ with increasing PSA concentrations from 0 to 80 ng mL^{-1}.*